Proc. 12th Int. Conf. on Hypernuclear and Strange Particle Physics (HYP2015)
JPS Conf. Proc. **17**, 101003 (2017)
https://doi.org/10.7566/JPSCP.17.101003

Hyperon mixing and universal many-body repulsion in neutron stars

Yasuo YAMAMOTO[1], Takenori FURUMOTO[2], Nobutoshi YASUTAKE[3], and Thomas RIJKEN[4]

[1]*Nishina Center for Accelerator-Based Science, Institute for Physical and Chemical Research (RIKEN), Wako, Saitama, 351-0198, Japan*
[2]*National Institute of Technology, Ichinoseki College, Ichinoseki, Iwate, 021-8511, Japan*
[3]*Department of Physics, Chiba Institute of Technology, 2-1-1 Shibazono Narashino, Chiba 275-0023, Japan*
[3]*IMAPP, University of Nijmegen, Nijmegen, The Netherlands*

E-mail: ys_yamamoto@riken.jp

(Received December 14, 2015)

Neutron stars with large masses $\sim 2M_\odot$ require the hard stiffness of equation of state (EoS) of neutron-star matter. On the other hand, hyperon mixing brings about remarkable softening of EoS. In order to solve this "Hyperon puzzle in neutron stars", a multi-pomeron exchange potential (MPP) is introduced as a model for the universal many-body repulsion in baryonic systems on the basis of the Extended Soft Core (ESC) baryon-baryon interaction. The strength of MPP is determined by analyzing the nucleus-nucleus scattering with the G-matrix folding model. The interactions in ΛN, ΣN and ΞN channels are shown to be consistent with experimental indications. The EoS in neutron-star matter with hyperon mixing is obtained from ESC in addition of MPP, and mass-radius relations of neutron stars are derived. The maximum mass is shown to reach $2M_\odot$ even in the case of including hyperon mixing by model-parameters determined by terrestrial experiments.

KEYWORDS: neutron star, EOS, hyperon mixing, hypernuclei ...

1. Introduction

The observed masses of neutron stars J1614-2230 [1] and J0348+0432 [2] are given as $(1.97 \pm 0.04)M_\odot$ and $(2.01 \pm 0.04)M_\odot$, respectively. These large masses give a severe condition for the stiffness of equation of state (EoS) of neutron-star matter. It is well known that the stiff EoS giving the maximum mass of $2M_\odot$ can be derived from the existence of strong three-nucleon repulsion (TNR) in the high-density region. However, the hyperon (Y) mixing in neutron-star matter brings about remarkable softening of the EoS, which cancels the TNR effect for the maximum mass [3]. One of ideas to avoid this "Hyperon puzzle in neutron stars" is to assume that the TNR-like repulsions work universally for YNN, YYN YYY as well as for NNN [3]. In our previous works [4], we introduced the multi-pomeron exchange potential (MPP) as a model of universal repulsions among three and four baryons on the basis of the Extended Soft Core (ESC) baryon-baryon interaction model developed by two of authors (T.R. and Y.Y.) and M.M. Nagels [5, 6].

Our approach is based on the Brueckner-Hartree-Fock (BHF) theory. Strength parameters of MPP are determined with no ad hoc parameter for the stiffness by using the result that the TNR effect appeared in the experimental angular distributions of ^{16}O+^{16}O elastic scattering (E/A=70 MeV) [9, 10]: Here, they analyzed successfully with the complex G-matrix folding potentials derived from ESC including MPP contributions, strengths of which were adjusted so as to reproduce the experimental data. Additionally to MPP, the three-nucleon attraction (TNA) is introduced phenomenologically so as to reproduce the nuclear saturation property. Our interaction model composed of ESC, MPP and

TNA is extended to hyperon channels: ESC gives potentials in $S = -1$ (ΛN, ΣN) and $S = -2$ (ΞN, $\Lambda\Lambda$ and $\Lambda\Sigma$) channels. MPP is universal in all BB channels according to its modeling. TNA defined phenomenologically in NN channels are extended so as to reproduce hypernuclear data in hyperonic channels; a three-baryon attraction (TBA). Using our BB interaction model (ESC+MPP+TBA), we derive the EoS of β-stable neutron-star matter composed of neutrons (n), protons (p), electrons (e^-), muons (μ^-) and hyperons (Λ, Σ^-, Ξ^-), and solve the Tolmann-Oppenheimer-Volkoff (TOV) equation for the hydrostatic structure to obtain mass-radius relations of neutron stars.

2. Neutron-star matter and EOS

We start the BB interaction model ESC, where all available NN-, YN-, and YY-data are fitted simultaneously with single sets of meson parameters. Here, two-meson and meson-pair exchanges are taken into account explicitly and no effective boson is included differently from the usual one-boson exchange models. The latest version of ESC model is named as ESC08c [6]. Hereafter, ESC means this version.

As a model of universal TBR, we introduce the multi-pomeron exchange potential (MPP) [4] consistently with the description of repulsive cores by pomeron exchange in ESC modeling. Generally, from the N-body local potential by pomeron exchange $W^{(N)}(\mathbf{x}_1, ..., \mathbf{x}_N)$ [4], the effective two-body potential in a baryonic medium is obtained by integrating over the coordinates $\mathbf{x}_3, ..., \mathbf{x}_N$. This gives

$$V^{(N)}_{eff}(\mathbf{x}_1, \mathbf{x}_2) = \rho^{N-2} \int d^3x_3 ... \int d^3x_N \; W^{(N)}(\mathbf{x}_1, \mathbf{x}_2, ..., \mathbf{x}_N)$$
$$= g_P^{(N)} g_P^N \frac{\rho^{N-2}}{\mathcal{M}^{3N-4}} \cdot \frac{1}{\pi\sqrt{\pi}} \left(\frac{m_P}{\sqrt{2}}\right)^3 \exp\left(-\frac{1}{2} m_P^2 r_{12}^2\right). \quad (1)$$

We assume that the dominant mechanism is triple and quartic pomeron exchange. The values of the two-body pomeron strength g_P and the pomeron mass m_P are the same as those in ESC. A scale mass $\mathcal{M}$ is taken as a proton mass.

In order to reproduce the nuclear saturation property, an adequate form of TNA must be added to ESC together with MPP. Here, we introduce TNA phenomenologically as a density-dependent two-body interaction

$$V_A(r;\rho) = V_0 \exp(-(r/2.0)^2) \rho \exp(-\eta\rho) (1 + P_r)/2 \,, \quad (2)$$

P_r being a space-exchange operator. V_0 and η are treated as adjustable parameters. $V_A(r;\rho)$ works only in even states due to the $(1 + P_r)$ factor. This assumption is needed to reproduce the ^{16}O+^{16}O potential at $E/A = 70$ MeV and nuclear-matter energy consistently [4].

Table I. Values of parameters included in MPP and TNA.

	$g_P^{(3)}$	$g_P^{(4)}$	V_0	η
MPa	2.34	30.0	−32.8	3.5
MPa$^+$	1.31	80.0	−21.6	1.0
MPb	2.94	0.0	−45.0	5.4

G-matrix calculations with the continuous (CON) choice are performed in nuclear matter, and G-matrix interactions are represented in coordinate space to construct nucleus-nucleus folding potentials [9]. In the same way as [4], the analyses for the ^{16}O+^{16}O elastic scattering at an incident energy

per nucleon $E_{in}/A = 70$ MeV are performed. The MPP strengths ($g_P^{(3)}$ and $g_P^{(4)}$) and the TNA parameters (V_0 and η) are determined to reproduce the scattering data using the G-matrix folding potential derived from ESC+MPP+TNA and nuclear-matter energy at saturation density. The calculated angular distributions of ^{16}O+^{16}O scattering are insensitive to the TNA parameters. Namely, it is essential in our approach that they are substantially determined by the MPP repulsive contributions in high density region [10]. On the other hand, they are not so dependent on a ratio of contributions of triple and quartic pomeron exchanges, and we can find various combinations of $g_P^{(3)}$ and $g_P^{(4)}$ reproducing the data equally well. As found in Eq.(1), the contributions from triple and quartic components are proportional to ρ and ρ^2, respectively. Therefore, the latter contribution play a remarkable role to stiffen the EoS in high density region. The chosen parameter sets are listed in Table I. These sets reproduces similarly the empirical values of energy per particle at saturation density, as well as symmetric energy and its slope parameter. The difference among these sets appear clearly in values of compressibility K: The saturation curve is fitted by a function $E/A = a\rho + b\rho^\gamma$ at $0.07 < \rho < 0.4$ fm^{-3}. The obtained values of K are 283, 313 and 254 MeV for MPa, MPa$^+$ and MPb, respectively, where the saturation points are the same value of $\rho_0 = 0.154$ fm^{-3}.

From the G-matrix calculations, we obtain the energy per nucleon E/A as a function of density ρ, being fitted by analytical functions. Then, energy density, chemical potential and pressure can be represented analytically.. Assuming a mixed matter of n, p, e^- and μ^- in chemical equilibrium, we solve the TOV equation. The obtained mass-radius relations of neutron stars are demonstrated in Fig.1. Solid, dashed and dotted curves are for MPa, MPa$^+$ and MPb, respectively. The EoS's in these cases are found to be stiff enough to give $2M_\odot$. The difference between MPa (MPa$^+$) and MPb is due to the quartic-pomeron exchange term included in the formers. The strengths of the effective two-body interaction derived from quartic-pomeron exchanges are proportional to ρ^2, and the contribution become sizeable in the high-density region, making the maximum mass large.

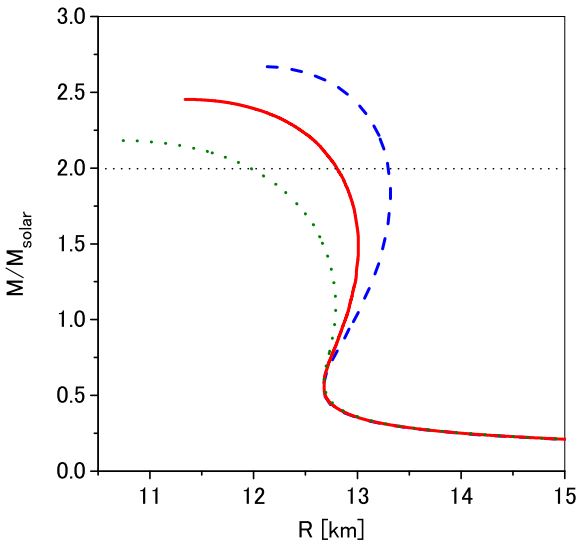

Fig. 1. Neutron-star masses as a function of the radius R.
Solid, dashed and dotted curves are for MPa, MPa$^+$ and MPb, respectively.

3. hyperon mixing in neutron stars

3.1 YN interaction

ESC gives potentials in $S = -1$ (ΛN, ΣN) and $S = -2$ (ΞN, $\Lambda\Lambda$ and $\Lambda\Sigma$) channels, being designed consistently with various data of *YN* scattering and hypernuclei. Then, the most important is to test the MPP+TBA parts in channels including hyperons. While MPP is defined universally in all baryon channel, TBA is introduced phenomenologically in nucleon channels, and not defined in *YN* channels. Then, it is necessary to determine the strength of TBA in each *YN* channel so as to reproduce the related hypernuclear data.

Table II. Values of U_Λ at normal density and partial wave contributions for MPa, MPa$^+$, MPb and ESC (in MeV). Values specified by P and D give sum of (S, J) contributions.

	$^1S_0$	$^3S_1$	P	D	U_Λ
MPa	−13.6	−25.9	4.1	−2.7	−38.1
MPa$^+$	−13.3	−25.1	4.3	−2.7	−36.9
MPb	−13.6	−26.0	4.1	−2.7	−38.3
ESC	−13.6	−25.3	1.1	−1.6	−39.4

In Fig.2, we show Λ binding energies in finite systems, calculated systematically with the Λ-nucleus folding potentials derived from finite-range G-matrix interactions $G_{\Lambda N}(r; k_F)$ for MPa (solid) and ESC (dashed) and the experimental data [7] were reproduced nicely. The similar result is obtained for MPb, while that for MPa$^+$ is a little smaller than the data.

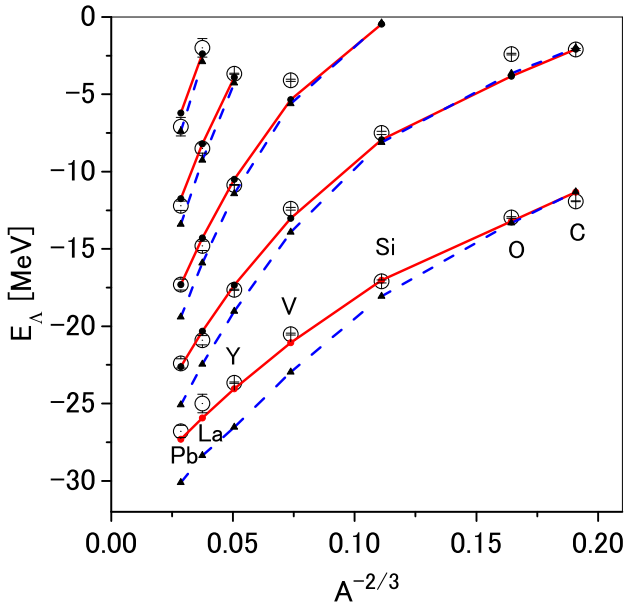

Fig. 2. Energy spectra of ${}^{13}_{\Lambda}$C, ${}^{28}_{\Lambda}$Si, ${}^{51}_{\Lambda}$V, ${}^{89}_{\Lambda}$Y, ${}^{139}_{\Lambda}$La and ${}^{208}_{\Lambda}$Pb are given as a function of $A^{-2/3}$, A being mass numbers of core nuclei. Solid (dashed) lines show calculated values by the G-matrix folding model derived from MPa (ESC).

In the case of ΛN case, such an assumption can be tested in detail by using the experimental data of Λ hypernuclei: We calculate ΛN G-matrices in symmetric nuclear matter including a single Λ hyperon. In Table II we show the potential energies U_Λ for a zero-momentum Λ and their partial-wave contributions in $^1S_0$, $^3S_1$, P and D states at normal density ρ_0 (k_F=1.35 fm^{-1}). Here, the TBA parts in MPa, MPa$^+$ and MPb are adjusted so that reasonable Λ binding energies are obtained. These three results including MPP+TBA are found to be similar to the ESC result, because MPP and TBA contributions are cancelled out substantially in normal density region in spite of remarkable difference in higher density region. One should be careful for comparing these values of $U_\Lambda(\rho_0)$ with the depth $U_{WS} \sim -30$ MeV of the Λ Woods-Saxon (WS) potential suitable to the data of Λ hypernuclei: In our approach, Λ binding energies in finite systems are reproduced by G-matrix folding potentials whose forms are considerably different from WS forms.

In Table III we show the potential energies $U_\Sigma(\rho_0)$ for a zero-momentum Σ and their partial-wave contributions for MPa, MPa$^+$, MPb and ESC. As well as the cases of $U_\Lambda(\rho_0)$, the results for MPa, MPa$^+$ and MPb are similar to the ESC result because of cancellations of MPP and TBA contributions in normal density region. It should be noted here that the strongly repulsive contributions in $T = 3/2$ $^3S_1$ and $T = 1/2$ $^1S_0$ states are due to the Pauli-forbidden effects in these states, being taken into account by strengthening the pomeron coupling in the ESC modeling. Especially, Σ^- potentials in neutron matter become strongly repulsive owing to $T = 3/2$ $^3S_1$ contributions. From the experimental data of Σ^- hypernuclear production, the Σ-nucleus potential is suggested to be strongly repulsive [8].

Table III. Values of U_Σ at normal density and partial wave contributions for MPa, MPa$^+$, MPb and ESC (in MeV). Values specified by P and D give sum of (S, J) contributions.

		$^1S_0$	$^3S_1$	P	D	U_Σ
MPa	$T = 1/2$	10.7	−23.1	−1.4	−1.0	
	$T = 3/2$	−13.3	30.4	0.1	−0.9	1.5
MPa$^+$	$T = 1/2$	10.6	−21.3	−1.4	−1.0	
	$T = 3/2$	−13.3	30.4	0.2	−0.9	3.4
MPb	$T = 1/2$	10.6	−23.2	−1.4	−1.0	
	$T = 3/2$	−13.3	30.3	0.1	−0.9	1.3
ESC	$T = 1/2$	10.9	−21.6	−2.5	−0.7	
	$T = 3/2$	−13.5	31.0	−2.1	−0.2	1.3

Table IV. Values of U_Ξ at normal density and partial wave contributions for MPa and ESC (in MeV). Values specified by P give sum of (S, J) contributions.

		$^1S_0$	$^3S_1$	P	U_Ξ
MPa	$T = 0$	1.0	−8.1	1.5	
	$T = 1$	9.7	−12.0	1.1	−6.7
ESC	$T = 0$	1.1	−8.0	0.9	
	$T = 1$	10.7	−10.8	−0.7	−6.8

Recently, it has been shown in [6] that the Ξ^- binding energies extracted from emulsion events of simultaneous emission of two Λ hypernuclei (twin Λ hypernuclei) [11] can be reproduced well

by the G-matrix interaction derived from ESC. In Table IV we show the potential energies $U_\Xi(\rho_0)$ for a zero-momentum Ξ and their partial-wave contributions for MPa and ESC. As well as the cases of Λ and Σ, the result for MPa is similar to that for ESC because of cancellations of MPP and TBA contributions in normal density region.

3.2 Hyperonic nuclear matter and EoS

We derive the EoS of baryonic matter composed of nucleons ($N = n, p$) and hyperons ($Y = \Lambda, \Sigma^-, \Xi^-$). A single particle potential of B particle in B' matter is given by

$$U_B(k) = \sum_{B'} U_B^{(B')}(k) = \sum_{B'} \sum_{k', k_F^{(B')}} \langle kk'|G_{BB',BB'}|kk'\rangle \tag{3}$$

with $B, B' = N, Y$. Here, spin isospin quantum numbers are implicit. The energy density is given by

$$\begin{aligned} \varepsilon &= \varepsilon_{mass} + \varepsilon_{kin} + \varepsilon_{pot} \\ &= 2\sum_B \int_0^{k_F^B} \frac{d^3k}{(2\pi)^3} \left\{ M_B + \frac{\hbar^2 k^2}{2M_B} + \frac{1}{2} U_B(k) \right\} \end{aligned} \tag{4}$$

The baryon number density is given as $\rho = \sum_B \rho_B$, ρ_B being that for component B. The chemical potentials μ_B and baryonic pressure P are expressed as

$$\mu_B = \frac{\partial \varepsilon}{\partial \rho_B} , \tag{5}$$

$$P = \rho^2 \frac{\partial(\varepsilon/\rho)}{\partial \rho} = \sum_B \mu_B \rho_B - \varepsilon . \tag{6}$$

Then, the G-matrix equations are solved for YN pairs ($Y = \Lambda, \Sigma, \Xi$) specified by isospin quantum numbers. The obtained isospin-represented YN G-matrices are transformed into those for Λn, Λp, $\Sigma^- n$, $\Sigma^- p$ and ΞN. Calculated values of energy densities are fitted by analytical functions.

We derive the EoS of neutron-star matter composed of n, p, e^-, μ^-, Λ, Σ^- and Ξ^-. The equilibrium conditions are given by (1) chemical equilibrium conditions, (2) charge neutrality, (3) baryon number conservation. When the analytical expressions are substituted into the chemical potentials (3), the chemical equilibrium conditions are represented as equations for densities ρ_a ($a = n$, p, e^-, μ^-, Λ, Σ^-, Ξ^-). Then, equations can be solved iteratively.

Here, for ΞN G-matrices we introduce an approximation for simplicity to replace them by ΞN-ΞN single-channel potentials, which are determined so as to simulate the results by coupled-channel G-matrix calculations at normal-density.

In left (right) panel of Fig.3, the matter compositions for MPa are shown in the case of without (with) Ξ^- mixing. Increasing of hyperon components are found to be covered by decreasing of components of n, e^- and μ^-.

Using the EoS of hyperonic nucleon matter, we solve the TOV equation to obtain the mass and radius of neutron stars. The EoS's for MPa, MPa$^+$ and MPb are used for $\rho > \rho_0$. Below ρ_0 we use the EoS of the crust obtained in [12, 13]. Then, the EoS's for $\rho > \rho_0$ and $\rho < \rho_0$ are connected smoothly. In left panel of Fig.4, the calculated values of pressure P are drawn as a function of baryon density ρ. Thick (thin) curves are with (without) hyperon mixing. In right panel of Fig.4, neutron-star masses are drawn as a function of radius R. In these figures, solid, dashed and dotted curves are for MPa, MPa$^+$ and MPb, respectively, where Ξ^- mixing is not taken into account. The cases of including Ξ^- mixing in both figures are shown by dot-dashed curves for MPa. Calculated values of maximum masses for MPa$^+$, MPa and MPb are $2.07M_\odot$, $1.94M_\odot$ and $1.83M_\odot$, respectively, being smaller by $0.61M_\odot$, $0.51M_\odot$ and $0.35M_\odot$, than the values without hyperon mixing. Although the universal repulsion works

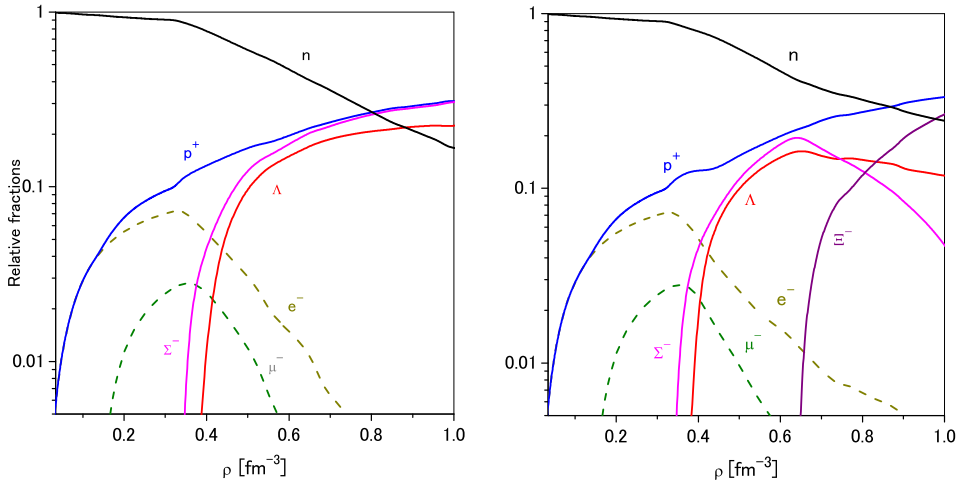

Fig. 3. Composition of hyperonic neutron-star matter for MPa. Left (Right) panel is without (with) Ξ^- mixing.

to raise the maximum mass, the hyperon mixing also is enhanced by it so that the maximum mass is reduced. This means that the universal repulsion cannot raise the maximum mass without limit. The maximum mass for MPb is considerably smaller than the observed value of $\sim 2M_\odot$. On the other hand, those for MPa and MPa$^+$ reach to this value owing to the four-body repulsive contributions.

The maximum mass is hardly changed by including Ξ^- mixing,, though Σ^- and Λ are replaced by Ξ^- gradually with increase of baryon density. The reason is because the universal repulsions (MPP) work equally to Λ, Σ^- and Ξ^-, being dominant contributions in high density region.

4. Conclusion

On the basis of the *BB* interaction model ESC, we introduce the universal three- and four-body repulsion MPP among baryons together with the phenomenological three-body attraction TBA. The strengths of MPP in nucleon channels are determined so as to fit the observed angular distribution of ^{16}O+^{16}O elastic scattering at $E_{in}/A = 70$ MeV with use of the G-matrix folding potential. The TBA parts are taken so as to assure the nuclear saturation property. Then, the stiff EoS of neutron-star matter without hyperon mixing is derived from the terrestrial experimental data, giving the large neutron-star mass over $2M_\odot$.

The EoS of hyperonic nuclear matter is obtained from ESC+MPP+TBA on the basis of the G-matrix approach, and the mass-radius relations of neutron stars are derived by solving the TOV equation. Though hyperon mixing leads to remarkable softening of the EoS, the stiffness is partially recovered owing to the MPP contribution. Quantitatively, in the case of MPb including only the three-body repulsion, the derived maximum mass is rather smaller than $2M_\odot$. In order to reproduce $2M_\odot$ clearly, the decisive roles are played by the four-body repulsions included in MPa and MPa$^+$. The effective two-body interactions derived from the three- and four-body repulsions are proportional to

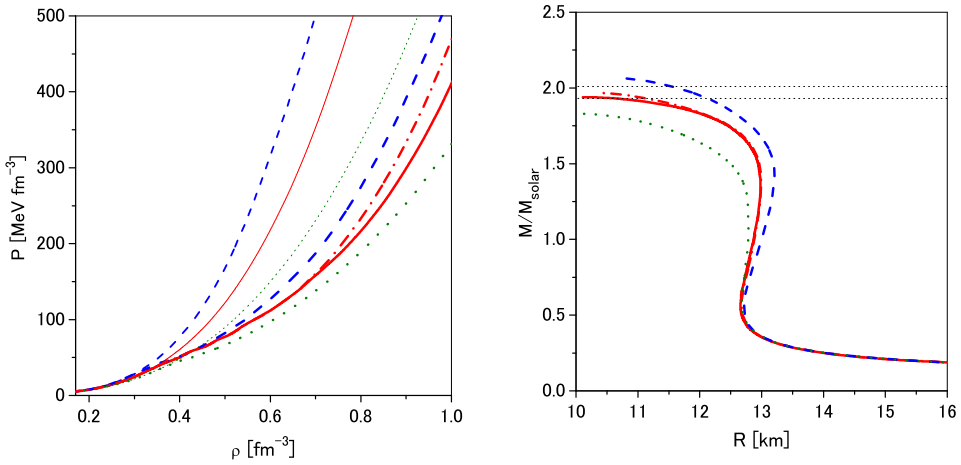

Fig. 4. Left panel: Pressure P as a function of baryon density ρ. Right panel: Neutron-star masses as a function of the radius R. Thick (thin) curves are with (without) hyperon mixing. Solid, dashed and dotted curves are for MPa, MPa$^+$ and MPb. Dot-dashed curve is in the case of including also Ξ^- mixing for MPa.

ρ and ρ^2, respectively. The latter contribution in high density region is sufficient to stiffen the EoS enough to give $2M_\odot$.

Our conclusion for neutron stars is obtained essentially on the basis of terrestrial experiments for nuclear and hypernuclear systems without using ad hoc parameters to stiffen the EoS. It can be said, at least, that our approach contributes to one of possible solutions of the hyperon puzzle.

References

[1] P.B. Demorest, T. Pennucci, S.M. Ransom, M.S.E. Roberts, and J.W. Hessels: Nature (London) **467**, (2010) 1081.
[2] J. Antoniadis *et al.*: Science **340**, (2013) 6131.
[3] S. Nishizaki, Y. Yamamoto, and T. Takatsuka: Prog. Theor. Phys. **105**, (2001) 607; **108**, (2002) 703.
[4] Y.Yamamoto, T.Furumoto, N.Yasutake and Th.A.Rijken: Phys. Rev. C**88**, (2013) 022801; C**90**, (2014) 045805; Eur. Phys. J. A **52** (2016) 19.
[5] Th.A. Rijken, M.M. Nagels, and Y. Yamamoto: Prog. Theor. Phys. Suppl. **185**, (2010) 14.
[6] M.M. Nagels, Th.A. Rijken, and Y. Yamamoto: arXiv:1408.4825 (2014); 1501.06636 (2015); 1504.02634 (2015).
[7] O.Hashimoto and H.Tamura: Prog. Part. Nucl. Phys. **57** (2006) 564.
[8] H. Noumi et. al.: Phys. Rev. Lett. **89** (2002) 072301.
[9] T. Furumoto, Y. Sakuragi, and Y. Yamamoto: Phys. Rev. C**79**, (2009) 011601(R); C**80**, (2009) 044614.
[10] T. Furumoto, Y. Sakuragi, and Y. Yamamoto: Phys. Rev. C**90**, (2014) 041601(R).
[11] K. Nakazawa *et al.*: Prog. Theor. Exp. Phys. **2015**, 033D02.
[12] G. Baym, A. Bethe, and C. Pethick: Nucl. Phys. A**175**, (1971) 225.
[13] G. Baym, C.J. Pethick, and P. Sutherland: Astrophys. J.**170**, (1971) 299.